Ratio of the interferon-γ signature to the immunosuppression signature predicts anti-PD-1 therapy response in melanoma

Yan Kong[1#], Canqiang Xu[2,4#], Chuanliang Cui[1#], Wenxian Yang[2], Shuang Yang[3], Zhihong Chi[1], Xinan Sheng[1], Lu Si[1], Yihong Xie[1], Jinyu Yu[1], Xuejun Chen[3], Shun Wang[2], Jing Hu[3], Frank Zheng[3], Wengang Zhou[3], Rongshan Yu[4*], Jun Guo[1*]

1. Peking University Cancer Hospital and Institute, Beijing, China

2. Aginome Scientific Co., Ltd., Xiamen, China

3. Amoy Diagnostics Co., Ltd., Shanghai, China

4. XMU-Aginome Joint Lab, School of Informatics, Xiamen University, China

# Y. K., C. X. and C.C. contributed equally to this work as first authors.

$*$ R.Y. and J.G. contributed equally to this work as senior authors.

Correspondence to: Rongshan Yu, Prof (rsyu@xmu.edu.cn) or Jun Guo, MD, PhD (guoj307@126.com).

Abstract

Immune checkpoint inhibitor (ICI) treatments produce clinical benefit in many patients. However, better pretreatment predictive biomarkers for ICI are still needed to help match individual patients to the treatment most likely to be of benefit. Existing gene expression profiling (GEP)-based biomarkers for ICI are primarily focused on measuring a T cell-inflamed tumour microenvironment

that contributes positively to the response to ICI. Here, we identified an immunosuppression signature (IMS) through analysing RNA sequencing data from a combined discovery cohort ($n = 120$) consisting of three publicly available melanoma datasets. Using the ratio of an established IFN-γ signature and IMS led to consistently better prediction of the ICI therapy outcome compared to a collection of nine published GEP signatures from the literature on a newly generated internal validation cohort ($n = 55$) and three published datasets of metastatic melanoma treated with anti-PD-1 ($n = 48$) and anti-CTLA-4 ($n = 42$) as well as in patients with gastric cancer treated with anti-PD-1 ($n = 45$), demonstrating the potential utility of IMS as a predictive/prognostic biomarker that complements existing GEP signatures for immunotherapy.

Key words: Immunology, immunotherapy, anti-PD-1, biomarker, tumour microenvironment, immune checkpoint inhibitor

1 Introduction

Historically, advanced melanoma has a poor prognosis, with a 5-year survival rate of less than 10%[1]. Immune checkpoint inhibitors (ICIs) targeting PD-1 and CTLA-4 have shown improved survival in advanced melanoma patients[1–4], but only a subset of patients respond. Additionally, the efficacy of ICIs has been observed to be significantly lower for East Asian melanoma patients than for Caucasian patients[5,6].

Published data suggest that tumour mutational burden (TMB) and PD-L1 expression may predict the clinical benefit of anti-PD-1 therapy in multiple cancer types[7–9]. Although the potential

predictive power of PD-L1 expression for the clinical benefit of anti-PD-1 therapy remains controversial for advanced melanoma patients[10,11], higher TMB has been correlated with a superior clinical response[12,13], improved survival[14,15], and durable benefit[12,16] in advanced melanomas. In Asian melanoma patients, acral[17,18] and mucosal melanomas[18] are the predominant subtypes and generally have a low point mutation burden. Consequently, it is not clear whether TMB is an effective predictor for advanced Asian melanoma patients.

In addition to TMB and PD-L1 expression, prediction models based on gene expression profiling (GEP) have also been proposed. Most GEP signatures consider T cell inflamed microenvironments characterized by the upregulation of IFN-γ signalling, antigen presentation, and immune checkpoint-related genes when predicting response to ICIs across multiple cancer types. However, these features are necessary but not always sufficient for a cancer patient to receive clinical benefit from ICI treatments[19]. A recent meta-review showed that predictive models built on inflamed GEP signatures achieved a moderate area under the receiver operator curve (AUC) value of 0.65 for the summary receiver operation characteristic (sROC) curve generated from 10 different solid tumour types in 8,135 patients[20].

Here, we argued that immune suppressive elements in the tumour microenvironment (TME) should be considered in combination with an inflamed GEP signature to more accurately predict ICI therapy outcomes. The main objective of this study was to develop immunosuppressive GEP signatures that, when used in combination with inflamed GEP signatures, could better stratify patients based on their potential benefits from ICI therapy. We started by analysing RNA-seq data

from baseline biopsy samples of melanoma patients treated with anti-PD-1 therapy and identified a set of 18 genes that played an "antagonistic" role against a pro-inflammatory TME and lead to negative outcomes in the discovery cohort consisting of multiple datasets. Our results reveal that key genes of the identified immunosuppression signature (IMS) are related to hallmark activities of cancer-associated fibroblasts (CAFs), macrophages and epithelial to mesenchymal transition (EMT), and the balance between the IFN-γ signature and the IMS plays an important prognostic and predictive role in both immunotherapy-naive primary tumours from The Cancer Genome Atlas (TCGA) database and ICI-treated patients.

2 Results

Definition of an immunosuppression signature. We reviewed the literature and found three external datasets[14,15,21] of advanced melanoma treated with an anti-PD-1 ICI with response and RNA-seq data, which we used as our discovery cohort ($n = 120$; Methods). We then identified 18 genes of which the expression levels, after adjusting for IFN-γ signature score, are consistently associated with negative response to ICI in the discovery cohort as our IMS (Fig. 1a-c). The genes in IMS with their respective biological functions are listed in Supplementary Table 1.

Fig. 1d shows a heatmap of the expression of all genes in the IMS and IFN-γ signatures in the combined discovery cohort. Patients with elevated expression of IFN-γ-related genes included both responders and nonresponders, suggesting that an inflamed TME alone, as indicated by a higher IFN-γ signature score, is not sufficient to ensure positive outcomes from ICI. On the other

hand, elevated expression levels of IMS genes were observed in patients from the nonresponder groups, particularly in the IFN-γ+ subgroup ($n = 49$, $p = 0.0006$). These data indicate a potential immunosuppressive role of the IMS genes that is opposite to the role of the IFN-γ related inflammatory signature, and both signatures should be considered in order to have more accurate predictions of outcomes from immunotherapy.

Association of the immunosuppression signature with immune cell types. The identified IMS shows a strong presence of genes related to CAFs (FAP and PDGFRB[22]) and tumour-associated macrophages (TAMs) (CD163[23] and SIGLEC1[24,25]) as well as their associated cytokines or chemokines that lead to an immunosuppressive microenvironment (IL10[26], CCL2, CCL8, and CCL13[14]) and stromal activities that lead to tumour proliferation, invasion and immune escape such as EMT or extracellular matrix (ECM) degradation (AXL[27], TWIST2, ADAM12[28], and COL6A3[29]). Therefore, high infiltration of CAFs and myeloid cells and their related stromal activities may be the reasons behind the lack of response from patients with an inflammatory TME. To further validate this hypothesis, we performed digital cell composition analysis using xCell[30] on a combined melanoma dataset consisting of the three datasets in the discovery cohort and a TCGA melanoma dataset ($n = 516$), and analysed the distribution of different immune cell types with respect to the IFN-γ signature and IMS scores.

As expected, we observed that the IMS score was positively correlated with the abundances of fibroblasts ($r = 0.62$, $p < 0.0001$), monocytes ($r = 0.45$, $p < 0.0001$) and macrophages ($r = 0.34$, $p < 0.0001$) (Fig. 2a). Stratification of patients into IFN-γ+/- and IMS+/- subgroups

according to their median values further revealed the different distributions of immune cells in relation to these two signatures (Fig. 2b). Fibroblasts were significantly enriched in IMS+ subgroups regardless of IFN-γ status ($p < 0.0001$; Fig. 2c). In addition, higher abundances of macrophage were associated with both higher IMS scores and higher IFN-γ signature scores. Interestingly, M2 macrophages, which play an important immunosuppressive role in the TME, were significantly associated with the IMS score in only the IFN-γ+ subgroups ($p = 0.0281$) but not the IFN-γ- subgroups. On the other hand, higher IFN-γ signature scores were associated with increased infiltration of CD8+ T cells, CD4+ T cells and B cells. However, the association of IMS scores and abundances of these cells within the microenvironment is not significant. All these results are consistent with the notion that IMS genes are related to immunosuppressive activities in cancers, and the balance between IFN-γ signature and IMS scores has a significant role in determining which patients benefit from adaptive immune rejuvating therapies.

Balance between the IFN-γ signature and the IMS as a biomarker for cancer. We next studied the distribution of IMS scores and their interaction with IFN-γ signature scores in different tumour types using TCGA data. First, we analysed the correlation between IMS scores and IFN-γ signature scores for all TCGA patients ($n = 11,043$; Fig. 3a). The results showed that the IFN-γ signature and IMS scores had a modest positive correlation with $r = 0.53$ ($p < 0.0001$); however, IMS scores were poorly explained by IFN-γ signature scores ($R^2 = 0.28$), suggesting that these two signatures are not fully overlapping and might contribute complementary information regarding the TME. A similar conclusion can be made on the correlation of the IMS and IFN-γ scores on selected cancer types from TCGA (Supplementary Fig. 1).

Given that the status of the tumour immune microenvironment and the associated composition of immune cells contain prognostic information, we hypothesized that the balance between IFN-γ signature and IMS may be associated with the survival of cancers. To assess this possibility, we performed a stratified multivariate analysis using Cox proportional hazards regression within each TCGA cancer type. The results showed that the association between the ratio of IFN-γ signature to the IMS score (IFN-γ/IMS) and overall survival (OS) varied according to cancer type (Fig. 3b). A higher IFN-γ/IMS ratio was associated with a modest prognostic benefit after adjusting for sex, age, and TMB in breast invasive carcinoma (BRCA) (HR = 0.93; 95% CI: 0.88 - 0.99), cutaneous melanoma (SKCM) (HR = 0.91, 95% CI: 0.84 - 0.98), stomach adenocarcinoma (STAD) (HR = 0.85; 95% CI: 0.76 - 0.94), and cervical tumours (CESC) (HR = 0.83; 95% CI: 0.73 - 0.96). Conversely, a higher IFN-γ/IMS ratio was associated with poor prognosis in uveal melanoma (UVM) (HR = 1.50; 95% CI: 1.07 - 2.11) and brain lower-grade gliomas (LGG) (HR = 1.41; 95% CI: 1.06 - 1.88), suggesting that these cancers may have different antitumour immune responses than those cancers mentioned previously. Interestingly, it was previously reported that a higher TMB was associated with poor survival in patients with glioma[7]. Associations of the IFN-γ/IMS ratio and survival in different directions have also been observed in other cancer types but did not reach statistical significance.

We further checked the relationship between the IFN-γ/IMS ratio and TMB scores in TCGA data and found that there was a positive but weak association between them ($r = 0.20$, $R^2 = 0.042$, $p < 0.0001$; Fig. 3b) on all samples from TCGA datasets ($n = 11,043$) and on selected cancer types (Supplementary Fig. 1).

Finally, we compared the median values of the IFN-γ signature score, the IMS score, and their ratio with objective response rates (ORRs) to anti-PD-1 therapies for cancer types with efficacy performance data available[31]. A positive correlation of ORR with the IFN-γ signature score ($R^2 = 0.27$, $p = 0.047$, Fig. 3e) and IFN-γ/IMS ($R^2 = 0.54$, $p = 0.001$, Fig. 3g) was observed (Fig. 3f). Importantly, tumours with high median IFN-γ/IMS values, most notably SKCM[32], colon adenocarcinoma (COAD), CESC[33], bladder urothelial carcinoma (BLCA)[34], lung squamous cell carcinoma (LUSC)[35] and liver hepatocellular carcinoma (LIHC), have shown clinical sensitivity to ICI therapies (Fig. 3g). Some tumour types (e.g., pancreatic adenocarcinoma (PAAD) and BRCA) have shown poor responses to immunotherapy despite their moderate to high median IFN-γ scores (Fig. 3e). These tumours are known to be highly infiltrated with myeloid cells, which may serve as an additional immunosuppressive mechanism preventing efficacy with ICI therapy[36,37]. Notably, these cancer types were also characterized by elevated IMS scores (Fig. 3c), and hence, a better association with ORR to ICI therapies was observed when both signatures were considered.

Ratio of the IFN-γ signature score to the IMS score predicts PD-1 blockade efficacy. We next assessed whether directly using the ratio of the IFN-γ signature score to the IMS score could be used as a reliable metric to predict anti-PD-1 therapy outcome for melanoma patients. We used IFN-γ/IMS together with the clinical response data to generate receiver operating characteristic (ROC) curves to quantify its prediction performance in our discovery cohorts. The resulting AUCs were in the range of 0.70 - 0.83 (Supplementary Fig. 3b).

We next tested the prediction ability of IFN-γ/IMS in a newly generated RNA-seq dataset

from 55 tumour tissues of melanoma patients treated with anti-PD-1 monotherapy at Peking University Cancer Hospital (PUCH), Beijing, China. In this dataset, IFN-γ/IMS achieved a prediction accuracy of AUC = 0.81 (95% CI: 0.69 - 0.93; Fig. 4e). Using the threshold that generated the maximum Youden index[38] to divide patients into predicted responder ($n = 29$) and predicted non-responder groups ($n = 26$), IFN-γ/IMS successfully captured 67.71% of nonresponders (23 out of 35) with only 3 exceptions (1 patient with a PR/CR and 2 patients with SD were misclassified as nonresponders), achieving a classification accuracy of 88.5% ($p = 0.0006$) for this group. On the other hand, of the 29 patients classified as predicted responders by IFN-γ/IMS, 17 (13 patients with a PR/CR and 4 patients with SD) actually responded. Overall, a higher IFN-γ/IMS ratio was associated with a better ORR ($p = 0.0005$; Fig. 4a), OS (HR = 2.78; 95% CI: 0.80 - 9.64; $p = 0.1214$; Fig. 4h) and progression free survival (PFS) (HR = 3.45; 95% CI: 0.97 - 12.19; $p = 0.0547$; Fig. 4g) than a lower IFN-γ/IMS ratio. Compared with IFN-γ signature-based classification (Fig. 4b), IFN-γ/IMS correctly classified six nonresponders that would otherwise be misclassified by IFN-γ signature as responders due to their medium to high IFN-γ scores, and one patient who had low IFN-γ score but responded to ICI therapy as responder (Fig. 4c). The OS and PFS results were not significant due to limited sample size, and relatively short follow-up period of this cohort. However, it was recently found that OS and PFS were significantly different between clinical responders and progressors of melanoma patients to anti-PD-1 therapy[13], suggesting that short-term response could be used as a surrogate for the survival benefits of patients in this context. In the public dataset of 48 preclinical metastasis melanoma treated with anti-PD-1 (Liu19[13]), IFN-γ/IMS achieved an AUC of 0.66 (95% CI: 0.50 - 0.83, Fig. 5b). In addition, patients with higher

IFN-γ/IMS ratio (with cutoff value based on the Youden index) had better ORR ($p = 0.0043$; Supplementary Fig. 2e) and longer PFS (HR = 4.36; 95% CI: 1.36 - 14.03; $p = 0.0013$, Fig. 5d). Collectively, the above data demonstrate the potential value of IFN-γ/IMS ratio as a combinatorial biomarker for anti-PD-1 treatment for metastastic melanoma.

Although the IMS was derived from advanced melanoma cohorts receiving anti-PD-1 treatment, the resulting genes measure immune-related expression levels with minimal contribution from tumour-related transcriptomic activities. Therefore, the signature may provide a treatment or tumour-type agnostic insight into immune microenvironment activities. To test this concept, we further evaluated the prediction performance of IFN-γ/IMS on two publicly available RNA-seq datasets with pretreatment samples from melanoma patients treated with anti-CTLA4 therapy (VanAllen15; $n = 42$)[39] and metastatic gastric cancer patients treated with anti-PD-1 therapy (Kim18; $n = 45$)[40]. The resulting AUCs were 0.75 (95% CI: 0.59 - 0.91; Fig. 5b) and 0.82 (95% CI: 0.64 - 0.99; Fig. 5b), respectively, for these two datasets. In addition, patients with high IFN-γ/IMS ratios (using the Youden index to determine the cutoff point) had better ORR on the VanAllen15 dataset ($p = 0.0004$; Supplementary Fig. 2d) and the Kim18 dataset ($p = 0.0022$; Supplementary Fig. 2f) and longer OS in the VanAllen15 dataset (HR = 3.06; 95% CI: 1.41 - 6.61; $p = 0.0032$; Fig. 5d) than patients with low IFN-γ/IMS ratios, suggesting the potential of using the IFN-γ/IMS ratio as a predictive/prognostic biomarker for immunotherapies different to anti-PD-1, or other cancer types.

Comparison with other GEP signatures.

Currently, there were significant number of independent studies on GEP signatures that predict the response of patients to anti-PD-1 therapy. To compare the prediction accuracy of the proposed IFN-γ/IMS ratio with that of existing GEP signature-based predictors, we generated predictions using nine published GEP signatures (Table 2) and the comparison results showed that IFN-γ/IMS ratio achieved better AUC performance on both PUCH (Fig. 4f) and the three external validation cohorts (Fig. 5c). One limitation of existing GEP signature studies is that many of these signatures were validated with independent cohorts within each publication, but frequently these signatures have not performed well in follow-up reports. To further validate the robustness of the proposed approach, we performed a randomized permutation test where three datasets were randomly selected from the seven datasets (Table 1) as the discovery cohort to identify the top 18 IMS genes as described previously. We then tested the prediction performance of ratio of IFN-γ and the identified IMS on the remaining four datasets. The results from the total 35 purmutation tests indicated that IFN-γ/IMS outperformed other GEP singatures by a significant margin (Wilcoxon matched-pairs signed rank test, $p < 0.0001$; Fig. 6a). Significantly, we found that the IMS signatures from the randomized tests were highly consistent despite that they were obtained from different training datasets. More than half of the total 630 occurrences of the IMS genes from the 35 randomized tests were from the top 23 frequent genes (Fig. 6b). Moreover, of the 18 IMS genes identified from the original discovery cohorts, 13 (OLFML2B, AXL, ADAM12, STC1, VCAN, PDGFRB, INHBA, CAT1, COL6A3, SIGLEC1, CD163, IL10, TWIST2) can be found in these top 23 frequent IMS genes from the randomized test. Further analysis of these genes on a public single-cell RNA-

seq (scRNA) dataset from melanoma[41] indicated that most of these genes are highly expressed on CAF (e.g., OLFML2B, VCAN, PDGFRB, COL6A3; Fig. 6d and Supplementary Fig. 4) and/or macrophages (e.g., VCAN, CD163, SIGLEC1; Fig. 6d and Supplementary Fig. 4), confirming the significant roles of these immune cells and their related immune suppressive activities in preventing patients from responding to anti-PD-1 therapy.

3 Discussion

There is significant interest in developing robust biomarkers of response to immunotherapy, as well as identifying actionable targets in those who do not respond to the current standard ICI therapies. Gene expression biomarkers, such as Oncotype DX[42], have demonstrated clinical utility in predicting treatment benefits in breast cancer. However, as interactions between the tumour and its microenvironment are highly complex, constructing predictors of patient response to ICIs remains a serious challenge.

Existing efforts to create gene expression-based tests for ICI efficacy have mainly focused on developing "response signatures" that measure the expression of adaptive immune response-related inflammatory genes[20], most of which include an IFN-γ gene signature as a major component[43]. However, due to the presence of intricate immunosuppressive mechanisms within the tumour microenvironment (TME), the presence of a peripherally suppressed adaptive immune response alone appears to be necessary but not sufficient for clinical benefit from PD-1/PD-L1 blockade. In this study, we identified an immunosuppression signature that, when combined with an inflammatory

signature, had prognostic/predictive value in patients with advanced melanoma treated with PD-1 blockade. To maximize our chance in identifying the correct genes for this signature, we started with an established 10-gene IFN-γ signature measuring the expression of genes associated with cytotoxic cells, antigen presentation, and IFN-γ activity[43] and then selected genes that were consistently upregulated in nonresponsive vs responsive groups after adjusting for the IFN-γ signature score based on their p-values on multiple datasets. In addition, since conceptually, a truly predictive gene should produce a significant result in all datasets, we used Pearson's method[44], which is more sensitive to the largest p-value, to combine p-values from different datasets to avoid artefacts due to single significance from individual dataset[45].

Strikingly, the genes identified in our IMS through the above computational method were highly consistent with several important biological activities related to innate or acquired resistance to ICIs. CAFs are a nonredundant, immunosuppressive component of the TME[46,47]. It was previously reported that INHBA production by cancer cells helps to induce CAFs, and ablating inhibin β A decreases the CAF phenotype both in vitro and in vivo[48]. CAFs hinder antitumour immunity by secreting immunosuppressive cytokines such as IL-10 and TGF-β, reducing CTL function and viability[49,50] and attracting immunosuppressive myeloid cells, including tumour-associated macrophage (TAMs), via CCL2[47,51]. Notably, SIGLEC1/CD163 is associated with the activation of macrophages towards an immunosuppressive phenotype, and accordingly, the expression of both CAF (FAP+) and TAM (SIGLEC1+) markers is associated with poor clinical outcomes across multiple tumour types[52–55]. CAF-mediated EMT, which is strongly correlated with the expression of AXL, TWIST2 and ADAM12 from the IMS, can result in biomechanical and biochem-

ical changes that facilitate tumour immune escape, invasion, and metastasis[56]. The dense collagen matrix produced by CAFs may also present a physical barrier to the infiltration of T lymphocytes[57] or treatments reaching the cancer cells[58]. Indeed, the association between a lack of response to ICIs and upregulated EMT-related genes has been observed in multiple cancers[40,59], and inhibiting CAF/TAM-related pathways and extracellular collagen and hyaluronan can induce T cell accumulation and improve the outcome of ICIs[60–63], reinforcing the role of those stromal-related activities in limiting the efficacy of immune checkpoint blockade immunotherapy.

Using the ratio of opposing immune signatures instead of the absolute value of individual signatures as a predictive/prognostic biomarker brings another advantage. It is well known that to compensate for potential technical variation, raw gene expression data from RNA-seq must be normalized so that meaningful biological comparisons can be made[64]. Typically, this is done with a set of housekeeping genes that are expected to maintain constant expression levels under different experimental conditions[65]. However, it has become increasingly clear that housekeeping gene expression levels may vary considerably in some conditions[66,67]. When that happens, the normalization process itself can lead to increased intersample "noise" that covers meaningful differences in target genes if the chosen housekeeping genes fluctuate randomly or erroneous results if there is a directional change in the housekeeping genes between experimental groups[66,68]. The calculation of the IFN-γ/IMS ratio provides a self-normalization method that directly measures the balance between contradicting biological processes within the tumour microenvironment, thus eliminating the need for using housekeeping genes that can be unreliable.

Our study has limitations. Since the current ICI clinical trials have generated gene expression data for only a limited number of pretreatment samples, which were insufficient to train robust prediction models, we did not systematically optimize the weights of individual genes in the IFN-γ/IMS ratio calculation. With more RNA-seq data available from subsequent studies, we expect that further optimization of the combined biomarker will yield even better predictive accuracy. In this study, we did not attempt to specify a universally applicable cutoff point for IFN-γ/IMS for different datasets due to potential batch effects from different RNA-seq procedures conducted at multiple sites. Rather, we demonstrated a trend that shows an increase in benefits with increasing IFN-γ/IMS ratios. Nevertheless, we envision that a relevant cutoff would need to be aligned to specific assay designs and clinical situations, and such a cutoff point could be further standardized based on additional evidence of merits from future clinical studies. Finally, our analysis is retrospective in nature, and validation of the findings in additional datasets is warranted.

In conclusion, the IMS studied in this paper exemplifies the potential of using GEP signatures for modeling the adverse TME, and using IMS in combination with an existing inflammatory GEP signature enables better identification of patients who could respond favorably to ICIs. Currently, clinical trials are assessing the efficacy of combining anti-PD-1 therapy with medicines that target at normalization of immune suppressive TME including the CSF1R inhibitor Cabrilizumab for the treatment of resectable biliary tract cancer (NCT03768531), CCR2 inhibitor plozalizumab for the treatment of melanoma (NCT02723006), the FAP inhibitor RO6874281 for the treatment of metastatic head and neck, oesophageal or cervical cancers (NCT03386721) and metastatic melanoma (NCT03875079), and the TGF-β inhibitor galunisertib (LY2157299) for the

treatment of advanced-stage NSCLC or hepatocellular carcinoma (NCT02423343) and metastatic pancreatic cancer (NCT02734160). However, due to the diversity of the immune evasion mechanisms in inflammatory tumours, such as loss of heterozygosity at the HLA locus[69], mutations in JAK-STAT signalling[70] or loss of IFN-γ pathway genes[71], reduced expression or loss of function of β2-microglobulin[72], and loss of immunogenic mutations[73] or epigenetic repression of neoantigen transcripts[74], specific immunosuppressive mechanisms utilized by each individual tumour would still need to be fully understood and gauged to better direct patients to different combination therapy options. In this regard, it is anticipated that IMS or future immunosuppressive signatures gleaning through deeper understanding of the immunosuppressive mechanisms of cancer would enable the development of more effective stratification models or therapeutic combinations to increase the efficacy and cost-effectiveness of immunotherapies for the benefits of cancer patients.

4 Methods

Patients and tissue samples. In this study, we obtained 55 formalin-fixed, paraffin-embedded (FFPE) tumour tissues from melanoma patients treated with anti-PD-1 monotherapy at PUCH, Beijing, China, between March 2016 and March 2019 (Supplementary Table 2). Diagnosis was histopathologically confirmed for all patients. Clinical data, including sex, age, tumour site, tumour thickness, metastasis status, and clinical efficacy, were collected. Therapy outcomes evaluated following Response Evaluation Criteria in Solid Tumors (RECIST) version 1.1, including presence of a complete or partial response (CR/PR), stable disease (SD) and progressive disease (PD), were used to assess efficacy. OS was calculated from the treatment start date. Patients who

did not die were censored at the date of last contact.

Whole-transcriptome RNA sequencing. Total RNA was extracted from unstained FFPE tumour samples by the All Prep-DNA/RNA-Micro Kit (Qiagen) following the standard manufacturer's protocol. Reverse transcription and second-strand cDNA synthesis were subsequently performed. Barcoded RNA libraries were generated and captured by a customized whole-exome panel. All libraries were sequenced on the Illumina NovaSeq 6000 platform with 2x150 bp paired-end reads. The mean sequencing coverage across all samples was $\sim$100X (3.5 G). RNA-seq reads were mapped to the human reference genome GRCh37 using STAR[75], and gene expression was quantified using RSEM[76]. Coding region reads were counted to calculate fragments per kilobase of transcript per million mapped reads (FPKM) values at the gene level and log2-transformed before analysis to avoid extremely skewed gene expression distributions.

External data sources. We collected the RNA-seq data of melanoma patients from six immunotherapy studies with gene expression profiles for pretreatment tumours and complete clinical information, including the Riaz17 ($n = 51$)[15], Hugo16 ($n = 28$)[14], Gide19 ($n = 41$)[21], VanAllen15 ($n = 42$)[39], Liu19 ($n = 54$)[13] and Kim18 ($n = 45$)[40] datasets (Table 1). Patients from these clinical studies were treated with nivolumab[15] and/or pembrolizumab[14,21]. For the Gide19 and Liu19 studies, only baseline data from samples that received anti-PD-1 monotherapy (nivolumab or pembrolizumab) were used. The immunotherapy outcomes provided in the original publications following RECIST guidelines (PR/CR/SD/PD) were used in our analysis. The gene expression data of VanAllen15 and Liu19 are download from respective references as provided by the authors. For

Riaz17, Hugo16, Gide19 and Kim18, the RNA-seq raw data was obtained and processed by the above mentioned pipeline to generate the gene expression data.

We downloaded TCGA Level-3 RSEM-normalized RNA-seq data and mutation packer calls from the TCGA database. The RNA-seq data were log2-transformed. Each patient's TMB was calculated as the number of nonsynonymous mutations.

Housekeeping normalization. We renormalized the RNA-seq data using a set of 20 reference ("housekeeping") genes (ABCF1, DNAJC14, ERCC3, G6PD, GUSB, MRPL19, NRDE2, OAZ1, POLR2A, PSMC4, PUM1, SDHA, SF3A1, STK11IP, TBC1D10B, TBP, TFRC, TLK2, TMUB2, and UBB) with low variance across a set of banked tumour samples from a variety of cancer types. The log2-transformed expression of each gene was normalized by subtracting the arithmetic mean of the log2-transformed expressions of the housekeeping genes.

Identification of the IMS genes. To identify the IMS genes, we performed a one-sided Student's t-test to capture genes that were systematically upregulated in the nonresponse groups (PD) vs response groups (PR/CR) after normalization by the IFN-γ signature score in each individual dataset. Due to the large dimensionality of the data, we restricted our search to the 770 cancer immune-related genes curated in Nanostring's IO 360 panel. The resulting p-values from the three datasets in the discovery cohort were combined using Pearson's method[44] to avoid artefacts due to single significance from individual dataset. The genes were ranked based on their Pearson combined p-values, and the top 18 genes were identified as our IMS genes.

Calculation of GEP signatures. We collected nine published GEP signatures related to the immune checkpoint response from the literature and validated in our cohorts (Table 2). Sample-wise scores of these signatures were calculated from RNA-seq data following the methodology described in the corresponding papers. Genes with unavailable expression data were excluded from the calculation of signature scores.

For the IFN-γ signature and IMS scores in this paper, we used the arithmetic mean of the log2-transformed, housekeeping gene normalized expression level of the 10-gene "preliminary" IFN-γ signature (IFNG, STAT1, CCR5, CXCL9, CXCL10, CXCL11, IDO1, PRF1, GZMA, and HLA-DRA)[43], and the 18 IMS genes listed in Supplementary Table 1 respectively. Furthermore, the IFN-γ signature/IMS ratio was calculated as the difference between these two scores in the logarithmic domain.

Single cell RNA-seq. Briefly, scRNA-seq data of 31 melanoma tumors were downloaded from GEO database (GSE115978)[41]. The original expression profiles and cell type annotations were used. Principal component analysis (PCA) was performed to reduce the dimensionality of the scRNA-seq profiles. Then t-SNE projections were generated using the first 25 principal components. Both PCA and t-SNE analysis were performed by RunPCA and RunTSNE functions in the Seurat package (version 3.1.0) with default parameters.

Data analysis and statistical information. Associations between categorical measurements and patient groups, such as the predictive accuracy of different biomarkers/panels, were evaluated using Fisher's exact test. Differences in continuous measurements were tested using the two-tailed

Mann-Whitney U-test. Correlations between two groups of continuous variables were evaluated using Pearson correlation analysis. The Kaplan-Meier method was utilized to estimate overall survival, and difference between groups were assessed using the log-rank test. Two-sided p-values were used unless otherwise specified, and a p-value less than 0.05 was considered significant. For boxplots, centre mark is median and whiskers are minimum/maximum unless specified otherwise.

PRISM was used for basic statistical analysis and plotting (http://www.graphpad.com), and the Python language and programming environment were used for the remainder of the statistical analysis. The abundances of multiple cell types in whole tissue samples were estimated using xCell[30].

Code availability. Codes are implemented in Python and are publicly available in GitHub: http://github.com/xxx.

Data availability. All patients data analysed from published papers are referenced to and publicly available accordingly. The gene expression data of patients from PUCH cohort will be deposited in the NCBI database once the manuscript is accepted for publishing. All the other data supporting the findings of this study are available within the article and its Supplementary Information files and from the corresponding author upon reasonable request.

DECLARATIONS

Funding. Grant No. 81672696, 81772912 and 81972557 from National Natural Science Foundation of China; Grant No. Z191100006619006 from the Beijing Municipal Science and Technology Commission; Clinical Plus X-Young Scholars Project (Peking University), the Fundamental Research Funds for the Central Universities and Beijing Baiqianwan Talents Project.

Study approval. The original studies were conducted in accordance with the Declaration of Helsinki and the International Conference on Harmonization Good Clinical Practice guidelines and approved by relevant regulatory and independent ethics committees from each study's institution. All patients provided written informed consent before study entry.

Authors' contributions. RY and JG designed the study; YK, CX and WY performed the data processing and machine learning analysis. CC, XS, LS, YX and JY collected tumour samples of patients and pooled clinical and survival data from Peking University Cancer Hospital. XC and SW performed the experiments; WX, SY, JH and WZ contributed to the analysis of the data; All authors contributed to the drafting and the revision of the manuscript.

Acknowledgements. We would like to thank Xu Xiao for her help in the analysis and visualization of the scRNA-seq data.

Conflict of interest statement. Jun Guo, the corresponding author, has the following consulting or advisory roles: MSD, Roche, Pfizer, Bayer, Novartis, Simcere Pharmaceutical Group, Shanghai

Junshi Biosciences, Oriengene.

Reference

1. F. Stephen Hodi, Steven J. O'Day, David F. McDermott, Robert W. Weber, Jeffrey A. Sosman, John B. Haanen, Rene Gonzalez, Caroline Robert, Dirk Schadendorf, Jessica C. Hassel, Wallace Akerley, Alfons J.M. Van Den Eertwegh, Jose Lutzky, Paul Lorigan, Julia M. Vaubel, Gerald P. Linette, David Hogg, Christian H. Ottensmeier, Celeste Lebbé, Christian Peschel, Ian Quirt, Joseph I. Clark, Jedd D. Wolchok, Jeffrey S. Weber, Jason Tian, Michael J. Yellin, Geoffrey M. Nichol, Axel Hoos, and Walter J. Urba. Improved survival with ipilimumab in patients with metastatic melanoma. *New England Journal of Medicine*, 363(8):711–723, 2010.

2. Jacob Schachter, Antoni Ribas, Georgina V. Long, Ana Arance, Jean Jacques Grob, Laurent Mortier, Adil Daud, Matteo S. Carlino, Catriona McNeil, Michal Lotem, James Larkin, Paul Lorigan, Bart Neyns, Christian Blank, Teresa M. Petrella, Omid Hamid, Honghong Zhou, Scot Ebbinghaus, Nageatte Ibrahim, and Caroline Robert. Pembrolizumab versus ipilimumab for advanced melanoma: final overall survival results of a multicentre, randomised, open-label phase 3 study (KEYNOTE-006). *The Lancet*, 390(10105):1853–1862, 2017.

3. Caroline Robert, Jacob Schachter, Georgina V. Long, Ana Arance, Jean Jacques Grob, Laurent Mortier, Adil Daud, Matteo S. Carlino, Catriona McNeil, Michal Lotem, James Larkin, Paul Lorigan, Bart Neyns, Christian U. Blank, Omid Hamid, Christine Mateus, Ronnie Shapira-Frommer, Michele Kosh, Honghong Zhou, Nageatte Ibrahim, Scot Ebbinghaus, and Antoni

Ribas. Pembrolizumab versus ipilimumab in advanced melanoma. *New England Journal of Medicine*, 372(26):2521–2532, 2015.

4. Caroline Robert, Antoni Ribas, Jacob Schachter, Ana Arance, Jean Jacques Grob, Laurent Mortier, Adil Daud, Matteo S. Carlino, Catriona M. McNeil, Michal Lotem, James M.G. Larkin, Paul Lorigan, Bart Neyns, Christian U. Blank, Teresa M. Petrella, Omid Hamid, Shu Chih Su, Clemens Krepler, Nageatte Ibrahim, and Georgina V. Long. Pembrolizumab versus ipilimumab in advanced melanoma (KEYNOTE-006): post-hoc 5-year results from an open-label, multicentre, randomised, controlled, phase 3 study. *The Lancet Oncology*, 20(9):1239–1251, 2019.

5. Lu Si, Xiaoshi Zhang, Yongqian Shu, Hongming Pan, Di Wu, Jiwei Liu, Fang Lou, Lili Mao, Xuan Wang, Xizhi Wen, Yanhong Gu, Lingjun Zhu, Shijie Lan, Xin Cai, Scott J. Diede, Yu Zhou, Jun Ge, Jianfeng Li, Haiyan Wu, and Jun Guo. A Phase Ib Study of Pembrolizumab as Second-Line Therapy for Chinese Patients With Advanced or Metastatic Melanoma (KEYNOTE-151). *Translational Oncology*, 12(6):828–835, 2019.

6. Naoya Yamazaki, Tatsuya Takenouchi, Manabu Fujimoto, Hironobu Ihn, Hiroshi Uchi, Takashi Inozume, Yoshio Kiyohara, Hisashi Uhara, Kazuhiko Nakagawa, Hiroshi Furukawa, Hidefumi Wada, Kazuo Noguchi, Takashi Shimamoto, and Kenji Yokota. Phase 1b study of pembrolizumab (MK-3475; anti-PD-1 monoclonal antibody) in Japanese patients with advanced melanoma (KEYNOTE-041). *Cancer Chemotherapy and Pharmacology*, 79(4):651–660, 2017.

7. Robert M. Samstein, Chung Han Lee, Alexander N. Shoushtari, Matthew D. Hellmann, Ronglai Shen, Yelena Y. Janjigian, David A. Barron, Ahmet Zehir, Emmet J. Jordan, Antonio Omuro, Thomas J. Kaley, Sviatoslav M. Kendall, Robert J. Motzer, A. Ari Hakimi, Martin H. Voss, Paul Russo, Jonathan Rosenberg, Gopa Iyer, Bernard H. Bochner, Dean F. Bajorin, Hikmat A. Al-Ahmadie, Jamie E. Chaft, Charles M. Rudin, Gregory J. Riely, Shrujal Baxi, Alan L. Ho, Richard J. Wong, David G. Pfister, Jedd D. Wolchok, Christopher A. Barker, Philip H. Gutin, Cameron W. Brennan, Viviane Tabar, Ingo K. Mellinghoff, Lisa M. DeAngelis, Charlotte E. Ariyan, Nancy Lee, William D. Tap, Mrinal M. Gounder, Sandra P. D'Angelo, Leonard Saltz, Zsofia K. Stadler, Howard I. Scher, Jose Baselga, Pedram Razavi, Christopher A. Klebanoff, Rona Yaeger, Neil H. Segal, Geoffrey Y. Ku, Ronald P. DeMatteo, Marc Ladanyi, Naiyer A. Rizvi, Michael F. Berger, Nadeem Riaz, David B. Solit, Timothy A. Chan, and Luc G.T. Morris. Tumor mutational load predicts survival after immunotherapy across multiple cancer types. *Nature Genetics*, 51(2):202–206, 2019.

8. Suzanne L. Topalian, F. Stephen Hodi, Julie R. Brahmer, Scott N. Gettinger, David C. Smith, David F. McDermott, John D. Powderly, Richard D. Carvajal, Jeffrey A. Sosman, Michael B. Atkins, Philip D. Leming, David R. Spigel, Scott J. Antonia, Leora Horn, Charles G. Drake, Drew M. Pardoll, Lieping Chen, William H. Sharfman, Robert A. Anders, Janis M. Taube, Tracee L. McMiller, Haiying Xu, Alan J. Korman, Maria Jure-Kunkel, Shruti Agrawal, Daniel McDonald, Georgia D. Kollia, Ashok Gupta, Jon M. Wigginton, and Mario Sznol. Safety, activity, and immune correlates of anti-PD-1 antibody in cancer. *New England Journal of Medicine*, 366(26):2443–2454, 2012.

9. Janis M Taube, Alison Klein, Julie R Brahmer, Haiying Xu, Xiaoyu Pan, and H Jung. Association of PD-1, PD-1 ligands, and other features of the tumor immune microenvironment with response to anti-PD-1 therapy. *Clin Cancer Res*, 20(19):5064–5074, 2014.

10. James Larkin, Vanna Chiarion-Sileni, Rene Gonzalez, Jean Jacques Grob, Christopher D Lao, Dirk Schadendorf, Reinhard Dummer, Michael Smylie, Piotr Rutkowski, Pier Francesco Ferrucci, Andrew Hill, John Wagstaff, Matteo S Carlino, Jedd D Wolchok, Stephen Hodi, and Dfciharvardedu Jdw. Combined Nivolumab and Ipilimumab or Monotherapy in Previously Untreated Melanoma. *N Engl J Med*, 373(1):23–34, 2015.

11. Bixia Tang, Xieqiao Yan, Xinan Sheng, Lu Si, Chuanliang Cui, Yan Kong, Lili Mao, Bin Lian, Xue Bai, Xuan Wang, Siming Li, Li Zhou, Jiayi Yu, Jie Dai, Kai Wang, Jinwei Hu, Lihou Dong, Haifeng Song, Hai Wu, Hui Feng, Sheng Yao, Zhihong Chi, and Jun Guo. Safety and clinical activity with an anti-PD-1 antibody JS001 in advanced melanoma or urologic cancer patients. *Journal of Hematology and Oncology*, 12(1):1–15, 2019.

12. Andrea Forschner, Florian Battke, Dirk Hadaschik, Martin Schulze, Stephanie Weißgraeber, Chung Ting Han, Maria Kopp, Maximilian Frick, Bernhard Klumpp, Nicola Tietze, Teresa Amaral, Peter Martus, Tobias Sinnberg, Thomas Eigentler, Ulrike Keim, Claus Garbe, Dennis Döcker, and Saskia Biskup. Tumor mutation burden and circulating tumor DNA in combined CTLA-4 and PD-1 antibody therapy in metastatic melanoma - Results of a prospective biomarker study. *Journal for ImmunoTherapy of Cancer*, 7(1):1–15, 2019.

13. David Liu, Bastian Schilling, Derek Liu, Antje Sucker, Elisabeth Livingstone, Livnat Jerby-

Amon, Lisa Zimmer, Ralf Gutzmer, Imke Satzger, Carmen Loquai, et al. Integrative molecular and clinical modeling of clinical outcomes to pd1 blockade in patients with metastatic melanoma. *Nature Medicine*, 25(12):1916–1927, 2019.

14. Willy Hugo, Jesse M Zaretsky, Lu Sun, Chunying Song, Blanca Homet Moreno, Siwen Hu-Lieskovan, Beata Berent-Maoz, Jia Pang, Bartosz Chmielowski, Grace Cherry, et al. Genomic and transcriptomic features of response to anti-pd-1 therapy in metastatic melanoma. *Cell*, 165(1):35–44, 2016.

15. Nadeem Riaz, Jonathan J Havel, Vladimir Makarov, Alexis Desrichard, William H Sharfman, Shailender Bhatia, Wen-jen Hwu, Thomas F Gajewski, and L Craig. Tumor and microenvironment evolution during immunotherapy with Nivolumab. *Cell*, 171(4):934–949, 2017.

16. Nicholas Mcgranahan, Andrew J S Furness, Rachel Rosenthal, Rikke Lyngaa, Sunil Kumar Saini, Mariam Jamal-hanjani, A Gareth, Nicolai J Birkbak, Crispin T Hiley, Thomas B K Watkins, Seema Shafi, Nirupa Murugaesu, Richard Mitter, Ayse U Akarca, Joseph Linares, Jake Y Henry, Eliezer M Van Allen, Diana Miao, and Bastian Schilling. Clonal neoantigens elicit T cell immunoreactivity and sensitivity to immune checkpoint blockade. *Science*, 351(6280):1463–1469, 2016.

17. Nicholas K. Hayward, James S. Wilmott, Nicola Waddell, Peter A. Johansson, Matthew A. Field, Katia Nones, Ann Marie Patch, Hojabr Kakavand, Ludmil B. Alexandrov, Hazel Burke, Valerie Jakrot, Stephen Kazakoff, Oliver Holmes, Conrad Leonard, Radhakrishnan Sabarinathan, Loris Mularoni, Scott Wood, Qinying Xu, Nick Waddell, Varsha Tembe, Guli-

etta M. Pupo, Ricardo De Paoli-Iseppi, Ricardo E. Vilain, Ping Shang, Loretta M.S. Lau, Rebecca A. Dagg, Sarah Jane Schramm, Antonia Pritchard, Ken Dutton-Regester, Felicity Newell, Anna Fitzgerald, Catherine A. Shang, Sean M. Grimmond, Hilda A. Pickett, Jean Y. Yang, Jonathan R. Stretch, Andreas Behren, Richard F. Kefford, Peter Hersey, Georgina V. Long, Jonathan Cebon, Mark Shackleton, Andrew J. Spillane, Robyn P.M. Saw, Núria López-Bigas, John V. Pearson, John F. Thompson, Richard A. Scolyer, and Graham J. Mann. Whole-genome landscapes of major melanoma subtypes. *Nature*, 545(7653):175–180, 2017.

18. Felicity Newell, Yan Kong, James S. Wilmott, Peter A. Johansson, Peter M. Ferguson, Chuanliang Cui, Zhongwu Li, Stephen H. Kazakoff, Hazel Burke, Tristan J. Dodds, Ann-Marie Patch, Katia Nones, Varsha Tembe, Ping Shang, Louise van der Weyden, Kim Wong, Oliver Holmes, Serigne Lo, Conrad Leonard, Scott Wood, Qinying Xu, Robert V. Rawson, Pamela Mukhopadhyay, Reinhard Dummer, Mitchell P. Levesque, Göran Jönsson, Xuan Wang, Iwei Yeh, Hong Wu, Nancy Joseph, Boris C. Bastian, Georgina V. Long, Andrew J. Spillane, Kerwin F. Shannon, John F. Thompson, Robyn P. M. Saw, David J. Adams, Lu Si, John V. Pearson, Nicholas K. Hayward, Nicola Waddell, Graham J. Mann, Jun Guo, and Richard A. Scolyer. Whole-genome landscape of mucosal melanoma reveals diverse drivers and therapeutic targets. *Nature Communications*, 10(1), 2019.

19. Flávia Castro, Ana Patrícia Cardoso, Raquel Madeira Gonçalves, Karine Serre, and Maria José Oliveira. Interferon-gamma at the crossroads of tumor immune surveillance or evasion. *Frontiers in Immunology*, 9(MAY):1–19, 2018.

20. Steve Lu, Julie E. Stein, David L. Rimm, Daphne W. Wang, J. Michael Bell, Douglas B.

Johnson, Jeffrey A. Sosman, Kurt A. Schalper, Robert A. Anders, Hao Wang, Clifford Hoyt, Drew M. Pardoll, Ludmila Danilova, and Janis M. Taube. Comparison of Biomarker Modalities for Predicting Response to PD-1/PD-L1 Checkpoint Blockade: A Systematic Review and Meta-analysis. *JAMA Oncology*, 5(8):1195–1204, 2019.

21. Tuba N. Gide, Camelia Quek, Alexander M. Menzies, Annie T. Tasker, Ping Shang, Jeff Holst, Jason Madore, Su Yin Lim, Rebecca Velickovic, Matthew Wongchenko, Yibing Yan, Serigne Lo, Matteo S. Carlino, Alexander Guminski, Robyn P.M. Saw, Angel Pang, Helen M. McGuire, Umaimainthan Palendira, John F. Thompson, Helen Rizos, Ines Pires da Silva, Marcel Batten, Richard A. Scolyer, Georgina V. Long, and James S. Wilmott. Distinct Immune Cell Populations Define Response to Anti-PD-1 Monotherapy and Anti-PD-1/Anti-CTLA-4 Combined Therapy. *Cancer Cell*, 35(2):238–255.e6, 2019.

22. Raghu Kalluri. The biology and function of fibroblasts in cancer. *Nature Reviews Cancer*, 16(9):582–598, 2016.

23. Alberto Mantovani, Federica Marchesi, Alberto Malesci, Luigi Laghi, and Paola Allavena. Tumour-associated macrophages as treatment targets in oncology. *Nature reviews Clinical oncology*, 14(7):399, 2017.

24. Kenichi Asano, Ami Nabeyama, Yasunobu Miyake, Chun-Hong Qiu, Ai Kurita, Michio Tomura, Osami Kanagawa, Shin-ichiro Fujii, and Masato Tanaka. Cd169-positive macrophages dominate antitumor immunity by crosspresenting dead cell-associated antigens. *Immunity*, 34(1):85–95, 2011.

25. Namir Shaabani, Vikas Duhan, Vishal Khairnar, Asmae Gassa, Rita Ferrer-Tur, Dieter Häussinger, Mike Recher, Gennadiy Zelinskyy, Jia Liu, Ulf Dittmer, et al. Cd169+ macrophages regulate pd-l1 expression via type i interferon and thereby prevent severe immunopathology after lcmv infection. *Cell death & disease*, 7(11):e2446–e2446, 2016.

26. Gerald Grütz. New insights into the molecular mechanism of interleukin-10-mediated immunosuppression. *Journal of leukocyte biology*, 77(1):3–15, 2005.

27. Carl M Gay, Kavitha Balaji, and Lauren Averett Byers. Giving axl the axe: targeting axl in human malignancy. *British journal of cancer*, 116(4):415–423, 2017.

28. Mark A Eckert, Miguel Santiago-Medina, Thinzar M Lwin, Jihoon Kim, Sara A Courtneidge, and Jing Yang. Adam12 induction by twist1 promotes tumor invasion and metastasis via regulation of invadopodia and focal adhesions. *Journal of cell science*, 130(12):2036–2048, 2017.

29. Peiwen Chen, Matilde Cescon, and Paolo Bonaldo. Collagen vi in cancer and its biological mechanisms. *Trends in molecular medicine*, 19(7):410–417, 2013.

30. Dvir Aran, Zicheng Hu, and Atul J Butte. xcell: digitally portraying the tissue cellular heterogeneity landscape. *Genome biology*, 18(1):220, 2017.

31. Mark Yarchoan, Lee A Albacker, Alexander C Hopkins, Meagan Montesion, Karthikeyan Murugesan, Teena T Vithayathil, Neeha Zaidi, Nilofer S Azad, Daniel A Laheru, Garrett M Frampton, et al. Pd-l1 expression and tumor mutational burden are independent biomarkers in most cancers. *JCI insight*, 4(6), 2019.

32. Suzanne L Topalian, Mario Sznol, David F McDermott, Harriet M Kluger, Richard D Carvajal, William H Sharfman, Julie R Brahmer, Donald P Lawrence, Michael B Atkins, John D Powderly, et al. Survival, durable tumor remission, and long-term safety in patients with advanced melanoma receiving nivolumab. *Journal of clinical oncology*, 32(10):1020, 2014.

33. Jan HM Schellens, Aurelien Marabelle, Susan Zeigenfuss, Jie Ding, Scott Knowles Pruitt, and Hyun Cheol Chung. Pembrolizumab for previously treated advanced cervical squamous cell cancer: preliminary results from the phase 2 keynote-158 study., 2017.

34. Thomas Powles, Peter H O'Donnell, Christophe Massard, Hendrik-Tobias Arkenau, Terence W Friedlander, Christopher J Hoimes, Jae Lyun Lee, Michael Ong, Srikala S Sridhar, Nicholas J Vogelzang, et al. Efficacy and safety of durvalumab in locally advanced or metastatic urothelial carcinoma: updated results from a phase 1/2 open-label study. *JAMA oncology*, 3(9):e172411–e172411, 2017.

35. Martin Reck, Delvys Rodríguez-Abreu, Andrew G Robinson, Rina Hui, Tibor Csőszi, Andrea Fülöp, Maya Gottfried, Nir Peled, Ali Tafreshi, Sinead Cuffe, et al. Pembrolizumab versus chemotherapy for pd-l1–positive non–small-cell lung cancer. *New England Journal of Medicine*, 375(19):1823–1833, 2016.

36. Stefano Ugel, Francesco De Sanctis, Susanna Mandruzzato, and Vincenzo Bronte. Tumor-induced myeloid deviation: when myeloid-derived suppressor cells meet tumor-associated macrophages. *The Journal of clinical investigation*, 125(9):3365–3376, 2015.

37. Neha Kamran, Mayuri Chandran, Pedro R Lowenstein, and Maria G Castro. Immature myeloid cells in the tumor microenvironment: Implications for immunotherapy. *Clinical Immunology*, 189:34–42, 2018.

38. W. J. Youden. Index for rating diagnostic tests. *Cancer*, 3(1):32–35, 1950.

39. Eliezer M. Van Allen, Diana Miao, Bastian Schilling, Sachet A. Shukla, Christian Blank, Lisa Zimmer, Antje Sucker, Uwe Hillen, Marnix H. Geukes Foppen, Simone M. Goldinger, Jochen Utikal, Jessica C. Hassel, Benjamin Weide, Katharina C. Kaehler, Carmen Loquai, Peter Mohr, Ralf Gutzmer, Reinhard Dummer, Stacey Gabriel, Catherine J. Wu, Dirk Schadendorf, and Levi A. Garraway. Genomic correlates of response to CTLA-4 blockade in metastatic melanoma. *Science*, 9(360):207–211, 2015.

40. Seung Tae Kim, Razvan Cristescu, Adam J. Bass, Kyoung-Mee Kim, Justin I. Odegaard, Kyung Kim, Xiao Qiao Liu, Xinwei Sher, Hun Jung, Mijin Lee, Sujin Lee, Se Hoon Park, Joon Oh Park, Young Suk Park, Ho Yeong Lim, Hyuk Lee, Mingew Choi, AmirAli Talasaz, Peter Soonmo Kang, Jonathan Cheng, Andrey Loboda, Jeeyun Lee, and Won Ki Kang. Comprehensive molecular characterization of clinical responses to PD-1 inhibition in metastatic gastric cancer. *Nature medicine*, 24(9):1449–1458, sep 2018.

41. Livnat Jerby-Arnon, Parin Shah, Michael S Cuoco, Christopher Rodman, Mei Ju Su, Johannes C Melms, Rachel Leeson, Abhay Kanodia, Shaolin Mei, Jia Ren Lin, and et al. A cancer cell program promotes t cell exclusion and resistance to checkpoint blockade. *Cell*, 175(4):984–997.e24, 2018.

42. Michelle Melisko. A multigene assay to predict recurrence of tamoxifen-treated, node-negative breast cancer. *Women's Oncology Review*, 5(1):45–47, 2005.

43. Mark Ayers, Jared Lunceford, Michael Nebozhyn, Erin Murphy, Andrey Loboda, Andrew Albright, David R. Kaufman, Jonathan D. Cheng, Veena Shankaran, Antoni Ribas, Tanguy Y. Seiwert, Terrill K. McClanahan, Jennifer Yearley, Sarina A. Piha-Paul, and S. Peter Kang. IFN-γ-related mRNA profile predicts clinical response to PD-1 blockade. *Journal of Clinical Investigation*, 127(8), 2017.

44. Karl Pearson. On a method of determining whether a sample of size n supposed to have been drawn from a parent population having a known probability integral has probably been drawn at random. *Biometrika*, pages 379–410, 1933.

45. Nicholas A Heard and Patrick Rubin-Delanchy. Choosing between methods of combining-values. *Biometrika*, 105(1):239–246, 2018.

46. Daniel S Chen and Ira Mellman. Elements of cancer immunity and the cancer–immune set point. *Nature*, 541(7637):321–330, 2017.

47. Lea Monteran and Neta Erez. The dark side of fibroblasts: cancer-associated fibroblasts as mediators of immunosuppression in the tumor microenvironment. *Frontiers in immunology*, 10:1835, 2019.

48. Archana S Nagaraja, Robert L Dood, Guillermo Armaiz-Pena, Yu Kang, Sherry Y Wu, Julie K Allen, Nicholas B Jennings, Lingegowda S Mangala, Sunila Pradeep, Yasmin Lyons, et al.

Adrenergic-mediated increases in inhba drive caf phenotype and collagens. *JCI insight*, 2(16), 2017.

49. Jake S O'Donnell, Michele WL Teng, and Mark J Smyth. Cancer immunoediting and resistance to t cell-based immunotherapy. *Nature reviews Clinical oncology*, 16(3):151–167, 2019.

50. Ana Costa, Yann Kieffer, Alix Scholer-Dahirel, Floriane Pelon, Brigitte Bourachot, Melissa Cardon, Philemon Sirven, Ilaria Magagna, Laetitia Fuhrmann, Charles Bernard, et al. Fibroblast heterogeneity and immunosuppressive environment in human breast cancer. *Cancer cell*, 33(3):463–479, 2018.

51. Linda Ziani, Salem Chouaib, and Jerome Thiery. Alteration of the antitumor immune response by cancer-associated fibroblasts. *Frontiers in immunology*, 9:414, 2018.

52. Woo J Lee, Mi H Lee, Hak T Kim, Chong H Won, Mi W Lee, Jee H Choi, and Sung E Chang. Prognostic significance of cd163 expression and its correlation with cyclooxygenase-2 and vascular endothelial growth factor expression in cutaneous melanoma. *Melanoma research*, 29(5):501–509, 2019.

53. Nobuyuki Fujii, Kohei Shomori, Tatsushi Shiomi, Motoki Nakabayashi, Chikako Takeda, Kazuo Ryoke, and Hisao Ito. Cancer-associated fibroblasts and cd163-positive macrophages in oral squamous cell carcinoma: their clinicopathological and prognostic significance. *Journal of oral pathology & medicine*, 41(6):444–451, 2012.

54. Mercedes Herrera, Alberto Herrera, Gemma Domínguez, Javier Silva, Vanesa García, José M García, Irene Gómez, Beatriz Soldevilla, Concepción Muñoz, Mariano Provencio, et al. Cancer-associated fibroblast and m2 macrophage markers together predict outcome in colorectal cancer patients. *Cancer science*, 104(4):437–444, 2013.

55. Yoshihiro Komohara, Masahisa Jinushi, and Motohiro Takeya. Clinical significance of macrophage heterogeneity in human malignant tumors. *Cancer science*, 105(1):1–8, 2014.

56. Freja A Venning, Lena Wullkopf, and Janine T Erler. Targeting ecm disrupts cancer progression. *Frontiers in oncology*, 5:224, 2015.

57. Hélène Salmon, Katarzyna Franciszkiewicz, Diane Damotte, Marie-Caroline Dieu-Nosjean, Pierre Validire, Alain Trautmann, Fathia Mami-Chouaib, and Emmanuel Donnadieu. Matrix architecture defines the preferential localization and migration of t cells into the stroma of human lung tumors. *The Journal of clinical investigation*, 122(3):899–910, 2012.

58. Patrice J Morin. Drug resistance and the microenvironment: nature and nurture. *Drug Resistance Updates*, 6(4):169–172, 2003.

59. Li Wang, Abdel Saci, Peter M. Szabo, Scott D. Chasalow, Mireia Castillo-Martin, Josep Domingo-Domenech, Arlene Siefker-Radtke, Padmanee Sharma, John P. Sfakianos, Yixuan Gong, Ana Dominguez-Andres, William K. Oh, David Mulholland, Alex Azrilevich, Liangyuan Hu, Carlos Cordon-Cardo, Hélène Salmon, Nina Bhardwaj, Jun Zhu, and Matthew D. Galsky. EMT- and stroma-related gene expression and resistance to PD-1 blockade in urothelial cancer. *Nature Communications*, 9(1), 2018.

60. Matthew Kraman, Paul J Bambrough, James N Arnold, Edward W Roberts, Lukasz Magiera, James O Jones, Aarthi Gopinathan, David A Tuveson, and Douglas T Fearon. Suppression of antitumor immunity by stromal cells expressing fibroblast activation protein–α. *Science*, 330(6005):827–830, 2010.

61. Christine Feig, James O Jones, Matthew Kraman, Richard JB Wells, Andrew Deonarine, Derek S Chan, Claire M Connell, Edward W Roberts, Qi Zhao, Otavia L Caballero, et al. Targeting cxcl12 from fap-expressing carcinoma-associated fibroblasts synergizes with anti–pd-l1 immunotherapy in pancreatic cancer. *Proceedings of the National Academy of Sciences*, 110(50):20212–20217, 2013.

62. Anders Etzerodt, Kyriaki Tsalkitzi, Maciej Maniecki, William Damsky, Marcello Delfini, Elodie Baudoin, Morgane Moulin, Marcus Bosenberg, Jonas Heilskov Graversen, Nathalie Auphan-Anezin, et al. Specific targeting of cd163+ tams mobilizes inflammatory monocytes and promotes t cell–mediated tumor regression. *Journal of Experimental Medicine*, 216(10):2394–2411, 2019.

63. Ivy X Chen, Vikash P Chauhan, Jessica Posada, Mei R Ng, Michelle W Wu, Pichet Adstamongkonkul, Peigen Huang, Neal Lindeman, Robert Langer, and Rakesh K Jain. Blocking cxcr4 alleviates desmoplasia, increases t-lymphocyte infiltration, and improves immunotherapy in metastatic breast cancer. *Proceedings of the National Academy of Sciences*, 116(10):4558–4566, 2019.

64. Eli Eisenberg and Erez Y Levanon. Human housekeeping genes, revisited. *TRENDS in Genetics*, 29(10):569–574, 2013.

65. William H Karge, Ernst J Schaefer, and Jose M Ordovas. Quantification of mrna by polymerase chain reaction (pcr) using an internal standard and a nonradioactive detection method. In *Lipoprotein Protocols*, pages 43–61. Springer, 1998.

66. Jeffrey T Leek, Robert B Scharpf, Héctor Corrada Bravo, David Simcha, Benjamin Langmead, W Evan Johnson, Donald Geman, Keith Baggerly, and Rafael A Irizarry. Tackling the widespread and critical impact of batch effects in high-throughput data. *Nature Reviews Genetics*, 11(10):733–739, 2010.

67. Peter D Lee, Robert Sladek, Celia MT Greenwood, and Thomas J Hudson. Control genes and variability: absence of ubiquitous reference transcripts in diverse mammalian expression studies. *Genome research*, 12(2):292–297, 2002.

68. Keertan Dheda, Jim F Huggett, Stephen A Bustin, Margaret A Johnson, Graham Rook, and Alimuddin Zumla. Validation of housekeeping genes for normalizing rna expression in real-time pcr. *Biotechniques*, 37(1):112–119, 2004.

69. Nicholas McGranahan, Rachel Rosenthal, Crispin T Hiley, Andrew J Rowan, Thomas BK Watkins, Gareth A Wilson, Nicolai J Birkbak, Selvaraju Veeriah, Peter Van Loo, Javier Herrero, et al. Allele-specific hla loss and immune escape in lung cancer evolution. *Cell*, 171(6):1259–1271, 2017.

70. Daniel Sanghoon Shin, Jesse M Zaretsky, Helena Escuin-Ordinas, Angel Garcia-Diaz, Siwen Hu-Lieskovan, Anusha Kalbasi, Catherine S Grasso, Willy Hugo, Salemiz Sandoval, Davis Y Torrejon, et al. Primary resistance to pd-1 blockade mediated by jak1/2 mutations. *Cancer discovery*, 7(2):188–201, 2017.

71. Jianjun Gao, Lewis Zhichang Shi, Hao Zhao, Jianfeng Chen, Liangwen Xiong, Qiuming He, Tenghui Chen, Jason Roszik, Chantale Bernatchez, Scott E Woodman, et al. Loss of ifn-γ pathway genes in tumor cells as a mechanism of resistance to anti-ctla-4 therapy. *Cell*, 167(2):397–404, 2016.

72. Nicholas P Restifo, Francesco M Marincola, Yutaka Kawakami, Jeff Taubenberger, John R Yannelli, and Steven A Rosenberg. Loss of functional beta2-microglobulin in metastatic melanomas from five patients receiving immunotherapy. *JNCI: Journal of the National Cancer Institute*, 88(2):100–108, 1996.

73. Maciej Kmieciak, Keith L Knutson, Catherine I Dumur, and Masoud H Manjili. Her-2/neu antigen loss and relapse of mammary carcinoma are actively induced by t cell-mediated anti-tumor immune responses. *European journal of immunology*, 37(3):675–685, 2007.

74. Rachel Rosenthal, Elizabeth Larose Cadieux, Roberto Salgado, Maise Al Bakir, David A Moore, Crispin T Hiley, Tom Lund, Miljana Tanić, James L Reading, Kroopa Joshi, et al. Neoantigen-directed immune escape in lung cancer evolution. *Nature*, 567(7749):479–485, 2019.

75. Alexander Dobin, Carrie A. Davis, Felix Schlesinger, Jorg Drenkow, Chris Zaleski, Sonali Jha, Philippe Batut, Mark Chaisson, and Thomas R. Gingeras. STAR: Ultrafast universal RNA-seq aligner. *Bioinformatics*, 29(1):15–21, 2013.

76. Bo Li and Colin N Dewey. RSEM: accurate transcript quantification from RNA-Seq data with or without a reference genome. *Bioinformatics*, 12(323), 2011.

77. Whijae Roh, Pei-Ling Chen, Alexandre Reuben, Christine N Spencer, Peter A Prieto, John P Miller, Vancheswaran Gopalakrishnan, Feng Wang, Zachary A Cooper, Sangeetha M Reddy, et al. Integrated molecular analysis of tumor biopsies on sequential ctla-4 and pd-1 blockade reveals markers of response and resistance. *Science translational medicine*, 9(379):eaah3560, 2017.

78. Jane L Messina, David A Fenstermacher, Steven Eschrich, Xiaotao Qu, Anders E Berglund, Mark C Lloyd, Michael J Schell, Vernon K Sondak, Jeffrey S Weber, and James J Mulé. 12-chemokine gene signature identifies lymph node-like structures in melanoma: potential for patient selection for immunotherapy? *Scientific reports*, 2:765, 2012.

79. Noam Auslander, Gao Zhang, Joo Sang Lee, Dennie T Frederick, Benchun Miao, Tabea Moll, Tian Tian, Zhi Wei, Sanna Madan, Ryan J Sullivan, Genevieve Boland, Keith Flaherty, Meenhard Herlyn, and Eytan Ruppin. Robust prediction of response to immune checkpoint blockade therapy in metastatic melanoma. *Nat Med*, 24(10):1545–1549, 2018.

80. Alexander C Huang, Robert J Orlowski, Xiaowei Xu, Rosemarie Mick, Sangeeth M George, Patrick K Yan, Sasikanth Manne, Adam A Kraya, Bradley Wubbenhorst, Liza Dorfman,

et al. A single dose of neoadjuvant pd-1 blockade predicts clinical outcomes in resectable melanoma. *Nature medicine*, 25(3):454–461, 2019.

81. Louis Fehrenbacher, Alexander Spira, Marcus Ballinger, Marcin Kowanetz, Johan Vansteenkiste, Julien Mazieres, Keunchil Park, David Smith, Angel Artal-Cortes, Conrad Lewanski, et al. Atezolizumab versus docetaxel for patients with previously treated non-small-cell lung cancer (poplar): a multicentre, open-label, phase 2 randomised controlled trial. *The Lancet*, 387(10030):1837–1846, 2016.

82. Teresa Davoli, Hajime Uno, Eric C Wooten, and Stephen J Elledge. Tumor aneuploidy correlates with markers of immune evasion and with reduced response to immunotherapy. *Science*, 355(6322):eaaf8399, 2017.

83. Michael S. Rooney, Sachet A. Shukla, Catherine J. Wu, Gad Getz, and Nir Hacohen. Molecular and genetic properties of tumors associated with local immune cytolytic activity. *Cell*, 160(1-2):48–61, 2015.

FIGURE LEGENDS

Fig. 1 | The definition of the IMS genes. a-c, Volcano plot depiction of differentially expressed genes after normalization by the IFN-γ score of individual sample by response on Riaz17 (in **a**, $n = 51$), Gide19 (in **b**, $n = 41$) and Hugo16 (in **c**, $n = 28$). R, responders (CR or PR); NR, nonresponders (PD) as per RECIST 1.1. IMS genes are highlighted in red. **d**, Heatmap showing the expression of genes from the IFN-γ signature and the IMS stratified by IFN-γ and response to

anti-PD-1 therapy. Rows represent genes and columns represent patients. The expression levels were z-normalized within rows for visualization. The cutoff value for the IFN-γ signature score was set to its median. **e**, The IMS scores in responders versus nonresponders for IFN-γ+ and IFN-γ- subgroups.

Fig. 2 | Association of IMS with abundance of immune cell types in TME. **a**- **b**, Heatmap showing the Pearson correlation of selected immune cell types with IMS scores (in **a**) and IFN-γ (in **b**) in combined melanoma cohorts consisting of all samples data from the discovery cohort and TCGA melanoma dataset ($n = 516$). Fibroblasts showed the strongest association with the IMS score (Pearson correlation $r = 0.62$, $p < 0.001$), followed by M1 macrophage ($r = 0.50$, $p < 0.001$), monocytes ($r = 0.45$, $p < 0.001$) and macrophage ($r = 0.35$, $p < 0.001$). On the other hand, CD8+ T-cell showed the strongest association with the IFN-γ score ($r = 0.61$, $p < 0.0001$). **c**, Violin plot showing the cell type distributions estimated using xCell for 4 groups of patients with IFN-γ+/IMS+ ($n = 183$), IFN-γ+/IMS- ($n = 75$), IFN-γ-/IMS+ ($n = 75$), IFG-γ-/IMS- ($n = 183$) in the combined melanoma cohort. Cutoff values for the IFN-γ signature and IMS scores were set to their median in all the data.

Fig. 3 | Balance between the INF-γ signature and IMS as a biomarker for cancer. **a**, Pearson correlations of IMS score with the IFN-γ signature ($r = 0.54$, $R^2 = 0.28$, $p < 0.0001$) for all TCGA patients ($n = 11,043$). **b**, Pearson correlation of logTMB with IFN-γ/IMS ratio ($r = 0.20$, $R^2 = 0.04$, $p < 0.0001$) for all TCGA patients ($n = 11,043$). **c**, Boxplots showing a summary of the distribution of IMS scores for all TCGA patients, with tumour types ordered by their me-

dian IMS score. **d**, Log hazard ratio estimates and 95% confidence intervals, with adjustment for sex, age, and TMB, with a binary cutoff (top 20% of each cancer type). Cancers in which the IFN-γ/IMS ratio was statistically significantly ($p < 0.05$) associated with good prognosis are highlighted in blue; significant associations with poor prognosis are in red. **e**-**g**, Associations of the ORR to immunotherapy for different cancer types with their median IFN-γ signature (linear regression goodness-of-fit $R^2 = 0.27$, $p = 0.381$; in **e**), IMS ($R^2 = 0.01$, $p = 0.715$; in **f**), and IFN-γ/IMS ($R^2 = 0.52$, $p = 0.017$; in **g**) values in the TCGA datasets.

Fig. 4 | Ratio of IFN-γ signature and IMS predicts response to ICI immunotherapy on the PUCH cohort. **a**, The ORR of patients from IFN-γ/IMS-high vs IFN-γ/IMS-low and **b** IFN-γ-high vs IFN-γ-low on the PUCH cohort. The cutoff points were decided by the Youden index for IFN-γ/IMS and IFN-γ scores, respectively. **c**, IFN-γ signature and IMS scores of individual patients in the PUCH cohort. The red and blue dashed lines indicate the cutoff points for IFN-γ/IMS ratio and IFN-γ, respectively. **d**, Waterfall plots of IFN-γ/IMS versus patients with different clinical responses to anti-PD-1 therapy in the PUCH cohort. **e**, ROC curve of the sensitivity versus 1-specificity of the predictive performance of IFN-γ/IMS. Patients with SD were not included in AUC calculation. **f**, Comparison of the AUC of IFN-γ/IMS with nine GEP signatures (Table 2) in predicting response to ICI. **g**, Kaplan-Meier plots of OS and PFS segregated by IFN-γ/IMS ratio with cutoff points selected according to the Youden index.

Fig. 5 | Ratio of IFN-γ signature and IMS predicts response to ICI immunotherapy on published datasets. **a**, Waterfall plots of the IFN-γ/IMS versus patients with different clinical re-

sponses to anti-PD-1 therapy in each validation cohort. **b**, ROC curve of the sensitivity versus 1-specificity of the predictive performance of IFN-γ/IMS. Patients with SD were not included in AUC calculation. **c**, Comparison of the AUC of IFN-γ/IMS with nine GEP signatures (Table 2) in predicting response to ICI. **d**, Kaplan-Meier plots of OS or PFS segregated by IFN-γ/IMS ratio with cutoff values selected according to the Youden index identified in individual datasets. Kaplan-Meier plot for Kim19 was not generated due to unavailability of survival data for this dataset.

Fig. 6 | Robustness of the proposed IMS signatures. **a**, Comparison of AUC performance of IFN-γ/IMS ratio with nine published GEP signatures (Table 2) after 35 bootstrapping randomized tests on the seven datasets (Table 1). In each randomized test, the IMS genes were identified from three randomly selected datasets (Methods), and the AUC prediction performance of the ratio of IFN-γ signature and the IMS identified from the randomly selected dataset was evaluated on the remaining four datasets. Models are sorted by their median AUC performances and Wilcoxon matched-pairs signed rank test was performed to compare the AUC performances of IFN-γ/IMS and the second best model T eff. **b**, Top 23 highly frequent genes from the bootstrapping tests. Genes in the original IMS signature are marked with an asterisk (*) symbol. **c-d**, t-SNE plot of cells from melanoma[41]. Cells are colored by cell types in (**c**) and by normalized expression of different IMS genes in (**d**).

Table 1: Cohorts used in this study

Cohort name	Tumour type	Cohort size	Target checkpoint
PUCH	Melanoma	55	PD-1
Riaz17[15]	Melanoma	51	PD-1
Gide19[21]	Melanoma	41	PD-1
Hugo16[14]	Melanoma	28	PD-1
VanAllen15[39]	Melanoma	42	CTLA-4
Liu19[13]	Melanoma	54	PD-1
Kim18[40]	Gastric	45	PD-1

Table 2: GEP signatures used in this study

Signature name	Number of genes	Description
IFN-γ/IMS	28	This work.
IFN-γ[43]	6	Averaging the expression levels of the IFN-γ signature genes.
Exp. Immu.[43]	18	Averaging the expression levels of the expanded immune genes.
Roh Immu.[77]	41	Averaging the expression levels of immune genes.
Messina[78]	12	Principal component 1 score from PCA of expression levels of 12 chemokine signature genes.
IMPRES[79]	28	Sum of ratios of 15 checkpoint or immune gene pairs.
Huang NRS[80]	69	Averaging the expression levels of neoadjuvant response signature (NRS) genes.
T eff.[81]	8	Averaging the expression levels of T-effector IFN-γ signature genes.
Davoli[82]	7	Averaging the expression levels of cytotoxic immune signature genes
Cytotoxic[83]	2	Averaging the expression levels of granzyme A (GZMA) and perforin (PRF1).

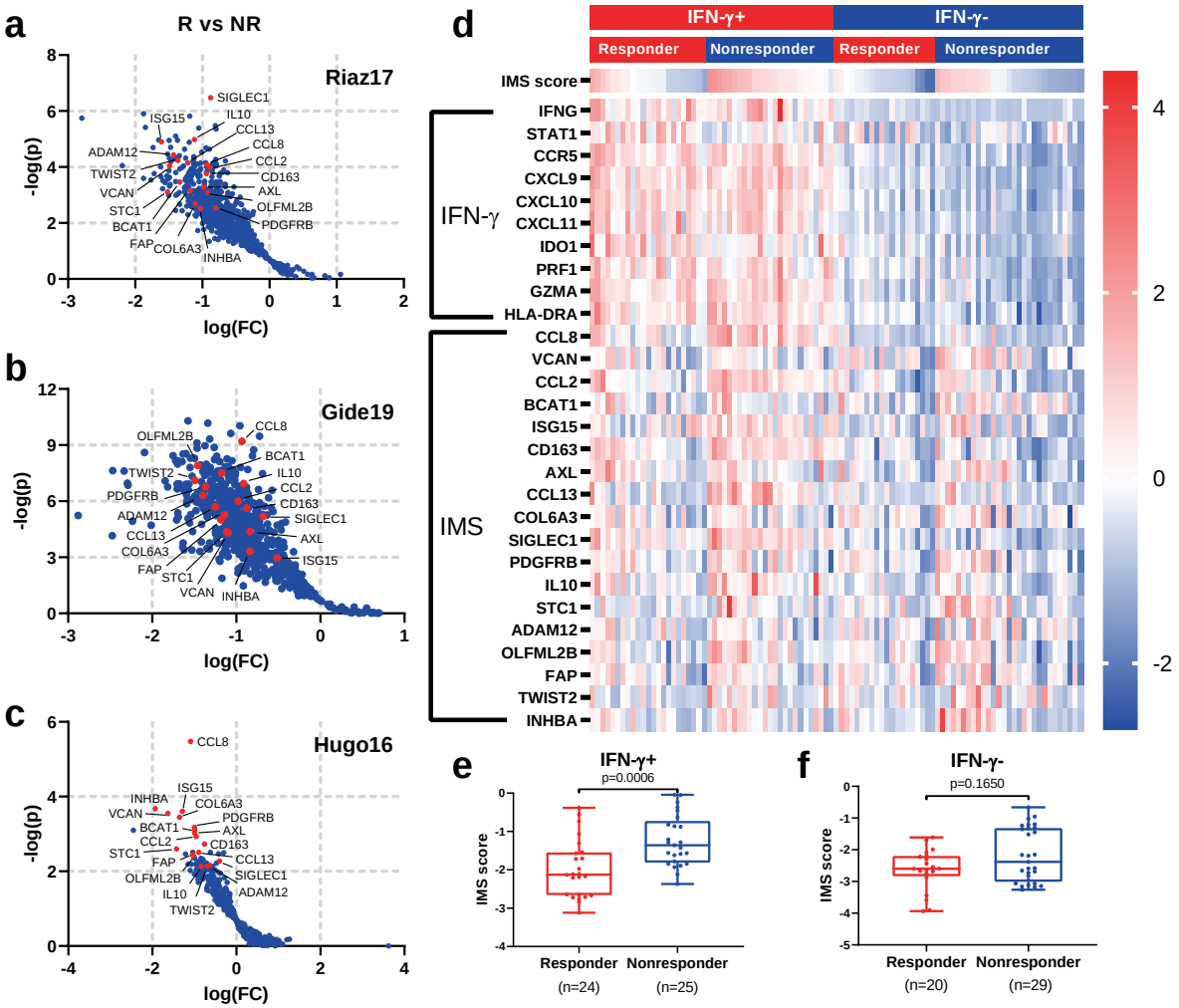

Figure 1:

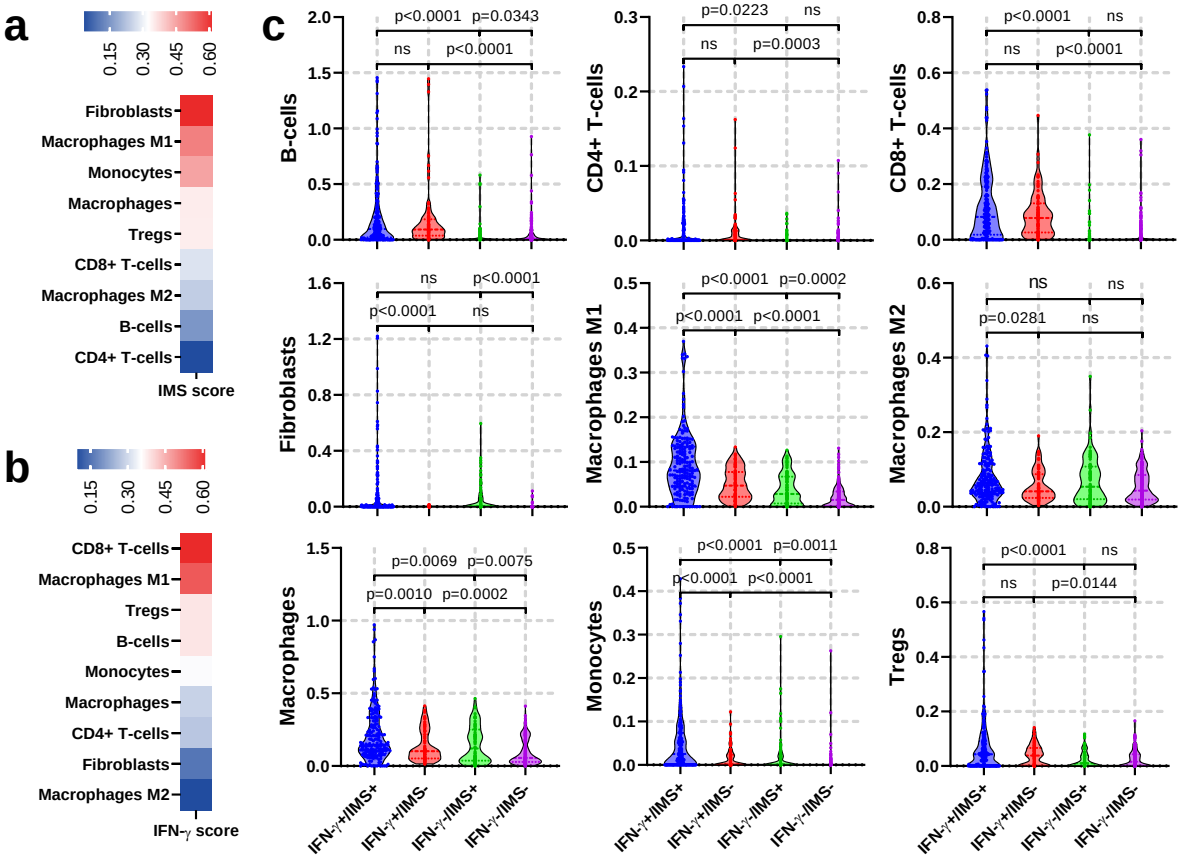

Figure 2:

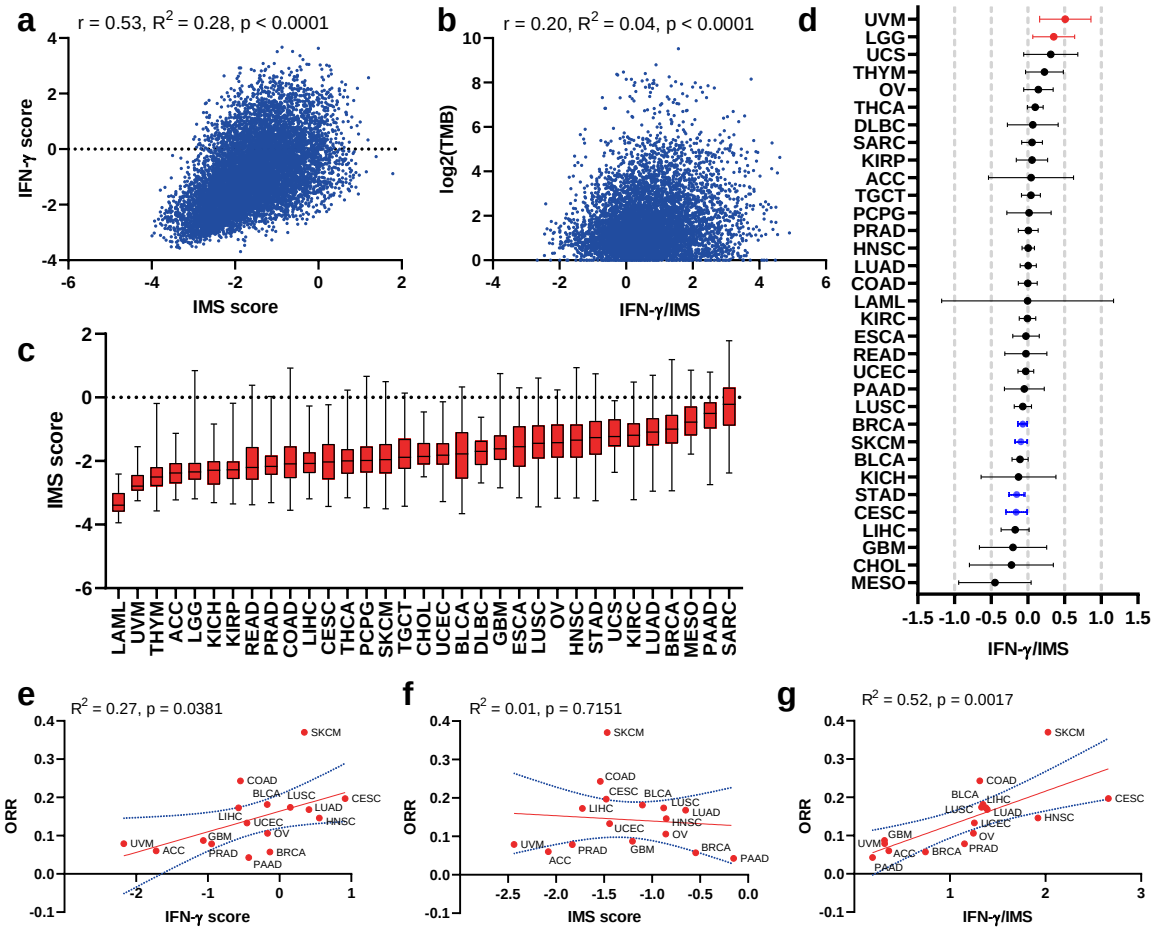

Figure 3:

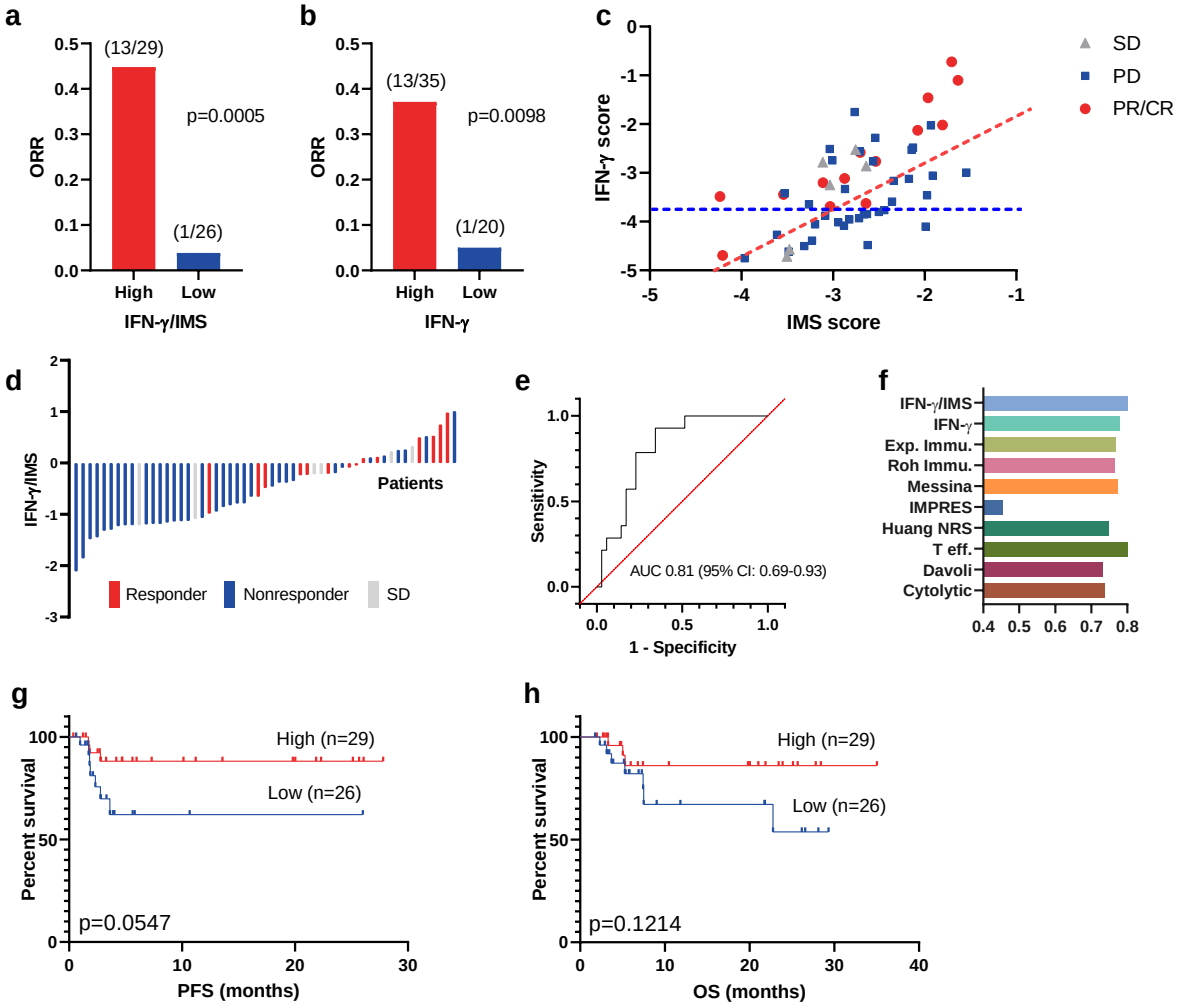

Figure 4:

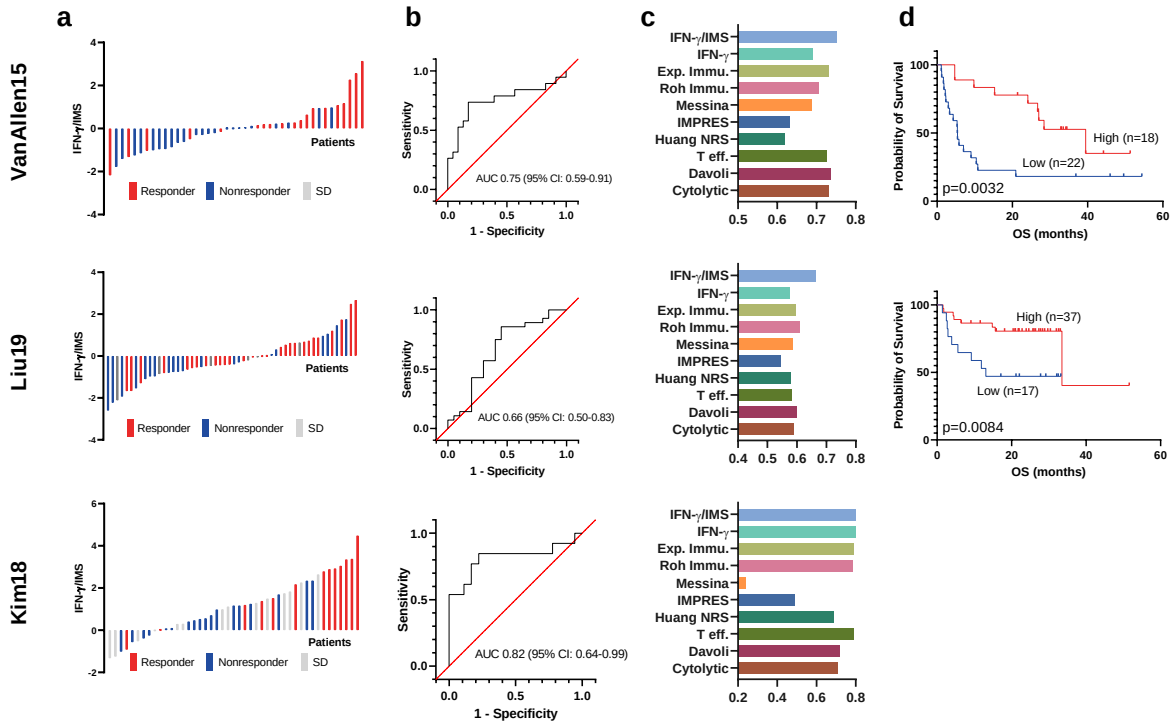

Figure 5: